# Performance Isolation for 5G RAN Slices while Managing Interference

Anonymous Author(s)

**Abstract.** Radio Access Network (RAN) slicing, a key 5G feature, enables different slices (i.e. tenants or applications) to share the same physical network infrastructure while pursuing diverse objectives such as fairness, prioritization, or maximizing throughput. Each slice is allocated a share of radio resource blocks (RBs), which it further schedules among its users as per its own performance objective. In this paper, we identify the unique challenges that arise when performing RAN slicing in today's multi-cell deployments that require a mechanism for managing interference among cells. We highlight how interference management decisions, that can be easily made in the absence of slicing (where all users share a common objective set by the network operator), become challenging with 5G slicing where we must respect the individual objectives of multiple slices, while retaining performance isolation across slices. We present a system, SiRAN, that tackles this challenge through a unique decision-making framework that allows different slices to independently contribute towards interference management decisions. SiRAN further employs a series of techniques to make such decisions within tight RAN scheduling budget of hundreds of microseconds. Trace-driven simulations with real-world channel measurements show that SiRAN improves slice-level objectives (e.g., throughput, fairness, flow completion times) by 20–60% over state-of-the-art baselines, while consistently meeting sub-millisecond decision deadlines.

## 1 Introduction

*Network slicing* [12, 23, 26, 42, 46] is a key architectural feature of 5G cellular networks. It enables cellular network operators divide their network resources among different "groups of users" or services (referred to as *slices*) as per by their respective SLAs (Service Level Agreements). Each slice then further sub-divides its share of resources among its own users as per its own policy or performance objective. In a way, 5G slicing crucially extends the notion of multi-tenancy to cellular networks, with each slice acting as a tenant. Examples of slices include mobile virtual network operators (MVNOs), such as GoogleFi [4] or Cricket [2], that leverage the physical infrastructure of network operators such as AT&T and Verizon to serve their own customers. A slice could also refer to a large enterprise managing multiple devices, or even specific applications (e.g. a team of drones doing city-wide sensing). These slices share the same physical infrastructure, while pursuing their own diverse performance objectives (e.g., fairness among all customers of an MVNO, maximizing throughput for a slice comprising a team of drones, an enterprising prioritizing certain users, etc). A key goal of slicing is to support such diverse performance objectives of each slice, while maintaining their SLAs, and ensuring performance isolation between slices.

Network slicing is particularly crucial at the Radio Access Network (RAN) where users across all slices share limited radio resources at a base-station. These radio resources are

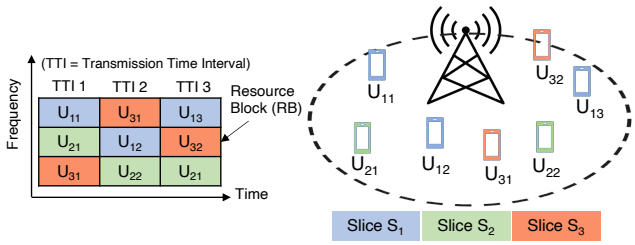


**Figure 1:** Radio resource blocks (RBs) at a base-station represented as a 2-D grid along time and frequency axes. The time slot spanning an RB is referred as a TTI. The RBs are scheduled across users belonging to different slices (three slices depicted in this example). User $U_{ij}$ belongs to slice $S_i$.

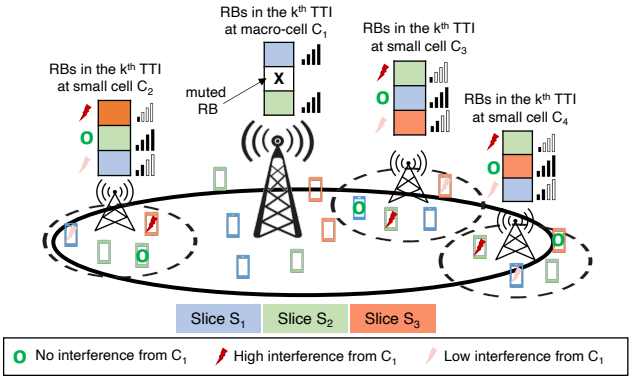


**Figure 2:** Typical multi-cell deployment with a macro-cell ($C_1$) and small cells ($C_2$, $C_3$, and $C_4$). The figure depicts how RBs at a given TTI are scheduled across users belonging to three different slices at each cell. Muting the transmission of an RB at a cell (say, the second RB at $C_1$, as shown) ensures that users scheduled on that RB at neighboring cells do not experience interference from $C_1$. The amount of interference from $C_1$ experienced by a user in a neighboring cell depends on the user's proximity to $C_1$, and impacts that user's *channel quality* (illustrated by the signal-strength bars).

split along the time and frequency axes into units called *resource blocks (RBs)*, as shown in Fig. 1. A user's performance (i.e. its throughput or datarate) depends on the amount of RBs assigned to it, as well as the quality of the wireless channel associated with those RBs. This channel quality (that determines the datarate per RB) depends on various factors including the user's distance from the base-station, obstacles, and potential interference from neighboring base-stations transmitting on the same frequency (i.e. on the same RB). A slice's SLA with the network operator governs its resource *quota*, i.e. number of RBs allocated to the slice at a base-station [18, 32]. The slice then schedules its allocated RBs across its users as per its own objective, taking the associated channel qualities into account.

RAN slicing has primarily been explored in the context of a single base-station (or cell) [18, 25, 33]. But today we are seeing a sharp increase in *multi-cell deployments* [7, 8], where the capacity and coverage of a single base-station (macro-cell) is scaled by deploying multiple *small* cells in its vicinity [11, 14, 15, 40, 44], as shown in Fig 2. Such multi-cell deployments are crucial for keeping up with increasing demands for cellular capacity. However, when two neighboring cells simultaneously transmit on the same frequency, the interference between them can severely degrade the channel quality (and, thereby, the throughput) of users in overlapping coverage regions. This necessitates some mechanism for interference management. Prior work has explored RAN slicing and interference management in isolation – but today's scale and applications demands require deploying both of them in tandem. In this paper, we identify and tackle the unique challenge that arises in such a setting – when we perform RAN slicing in conjunction with interference management in multi-cell deployments.

To understand the challenge, let us first consider how interference can be managed without any slicing, where all users share a single global objective set by the network operator (typically proportional fairness among all users). Interference management in such a "no slicing" setting has been explored by prior work [47, 50, 56]. A common strategy is to mute the transmission of certain cells on specific RBs [10, 27, 45]. As depicted in Fig 2, muting the transmission of an RB (say the second RB at macro-cell $C_1$ in our example) ensures that users at other cells scheduled on that RB do not experience any interference from $C_1$. Deciding whether or not to mute an RB $r$ on a cell $C$ requires weighing the cost of muting incurred by users at cell $C$ (due to unavailability of muted RBs) versus its benefit enjoyed by users at cells neighboring $C$ (due to boosted channel quality caused by reduced interference). It is relatively straightforward to reason about such a trade-off without slicing. The benefit vs. cost of a muting decision can be analyzed based on whether or not it improves the network operator's global objective.

However, with 5G slicing, cellular users do not share a single global objective. Instead, each slice optimizes for its own objective, which is incomparable with other slices' objectives. The decision to mute RB $r$ on a cell $C$ might seemingly benefit a user of slice $S_i$ at a neighboring cell, but hurt a user of another slice $S_j$ (which would have otherwise been scheduled on RB $r$ at cell $C$) hence violating the performance isolation promised by slicing. So then how do we reason about such a muting decision while supporting diverse slice objectives, and without violating performance isolation across slices?

Our system, SiRAN, addresses this challenge by introducing a unique form of cost-benefit analysis that allows slices to *independently contribute* towards a muting decision based on their own objectives, without hurting the performance of any other slice. SiRAN restricts the penalty of muting an RB at a cell $C$ to the $K$ slices that benefit from the muting decision, by reducing each of their quotas at cell $C$ by $1/K$ RBs. This enables us to assess the cost (reduced quota at cell $C$) versus the benefit (reduced interference at nearby cells) independently for each of the $K$ slices as per the slice's objective. The slice pays the penalty only if the muting decision improves its objective. SiRAN mutes this RB at cell $C$ only if one or more slices are willing to pay the penalty.

SiRAN must tackle multiple challenges to realize this approach. The first challenge is identifying the set of $K$ slices for which the benefits of muting the RB outweigh the costs. The cost incurred by a slice ($1/K$ RBs) depends on the number of benefiting slices $K$ itself, creating a chicken-and-egg problem. SiRAN tackles this through an iterative approach – starting with an initial set of slices that presumably benefit from the muting decision, and repeatedly updating the set after conducting the cost-benefit analysis for each such slice.

The second challenge stems from the fact that muting decisions are inter-twined with scheduling decisions – whether or not an RB at a cell is muted influences the channel quality (and therefore the scheduling decision) on that RB at neighboring cells. The changes in slice quotas caused by a muting/scheduling decision for an RB further has a ripple effect on how the *subsequent* RBs at each cell are scheduled. Therefore, in order to accurately assess the cost and benefit of muting an RB, SiRAN must ideally re-run the scheduler for all the remaining RBs at each cell. However, doing so is prohibitively expensive – the joint muting and scheduling decisions must be made within tight time slots (i.e. within a TTI, which ranges from 250$\mu$s to 1ms in 5G). SiRAN handles this challenge by employing a series of techniques that effectively approximate the benefit and cost of a muting decision without re-running the scheduler, as detailed in §4. Our approximation techniques also help tackle a third challenge – computing the penalty of reducing a slice's quota by a fraction of an RB (despite the fact that RBs are allocated to users as a whole and cannot be split).

We implement SiRAN in an open-source RAN simulator [43] and collect real-world traces to perform trace-driven evaluations in §6. Our evaluation, across a variety of realistic scenarios spanning hundreds of users split across multiple slices with diverse objectives, shows how SiRAN results in 20-60% improvement in the performance of individual slices (on their desired performance objective) when compared to several baselines. Our comparative baselines include (i) a RAN slicing system that independently schedules RBs at each cell without any interference management or muting [18], (ii) a baseline that makes its muting decision based on a single shared objective [10, 27, 45], ignoring the individual objectives of each slice, and (iii) a strawman approach to enable interference management with slicing [21] that we detail in §2. Our evaluation further shows how the approximation techniques employed by SiRAN reduce the computation overhead by orders of magnitude, enabling it to make its muting decisions within stringent scheduling time budgets of $\leq 1$ ms, without compromising on their correctness.

# 2 Background and Related Work

## 2.1 Radio Access Network (RAN)

Radio Access Network (RAN) refers to the wireless last-mile of cellular networks, connecting the base-station to the end-devices (referred as user equipments or UEs). We explain some relevant RAN concepts below.

**Resource Block.** RAN resources are divided along the frequency and time axes. Specifically, the frequency bandwidth of the radio spectrum is divided into multiple sub-carrier frequencies, and time is divided into equal slots called TTIs (Transmission Time Intervals). In 5G, a TTI slot can range from 250$\mu$s-1ms [24]. A resource block (RB) is formed of 12 frequency sub-carriers and 1 TTI slot, and is the smallest resource unit that can be allocated to a user. We can thus visualize the RBs as being organized into a 2D grid as shown in Fig. 1. For simplicity, the figure depicts RBs as the scheduling granularity across users. In practice, network operators schedule radio resources in the granularity of resource block groups (RBGs) to reduce control overhead. Each RBG contains a fixed number of consecutive RBs ranging from 2 to 16 [24, 48]. Henceforth, we will use the term RBG to refer to the scheduling granularity of radio resources across users.

**Channel Quality and User Performance.** The performance of a user (i.e. how much throughput or data rate they achieve) depends on the number of RBGs assigned to them and the *channel quality* associated with those RBGs (higher channel quality results in a higher data rate per RBG). Typically, the closer the user is to a base-station, the higher is its channel quality. However, obstacles or interference from neighboring base-stations can introduce noise in the signal and degrade the channel quality. Different users (in different locations) can thus experience drastically different channel quality for the same RBG. Moreover, a given user can also see a high variation in channel quality across RBGs, even within the same TTI, due to a phenomenon called frequency selective fading. The combination of these factors motivates the need for incorporating channel awareness when scheduling radio resources across users [17, 18]. The user equipment (UE) periodically reports its channel quality to the base station to enable channel-aware scheduling. We provide a brief primer on channel-aware scheduling mechanisms in §3.1.

## 2.2 RAN Slicing

As mentioned in §1, RAN slicing is a key 5G feature that brings the notion of multi-tenancy to cellular networks. With RAN slicing, the network operator (e.g. AT&T, Verizon, etc) divide the radio resources among heterogeneous slices (MVNOs, enterprises, applications, etc) as per their SLAs. The SLA of a slice translates to a minimum *quota* of RBGs that the network operator must allocate to it at a base-station [18, 32]. Each slice then schedules its quota of radio resources across its own users as per its own performance objective (e.g. fairness, prioritization, throughput maximization, etc). The performance objective typically varies across slices. A slicing system must support such diverse slice objectives, and ensure each slice gets its quota of resources while retaining performance isolation across slices.

Prior work on RAN slicing has largely been restricted to scheduling radio resources at a single base-station (e.g. [3, 18, 25, 32]). Other works [16, 38] look at the problem of mapping network-wide service-level agreements (SLAs) to per-cell resource quotas for a given slice but ignore potential interference across cells. We leverage these prior works for determining per-cell slice quotas and doing channel-aware slicing and scheduling [18] (as detailed in §3.1). The primary focus of our work, however, is to address the challenges that arise from the interplay of RAN slicing with interference management across multiple cells.

## 2.3 Multi-Cell Deployments

As depicted in Fig. 2, network operators commonly scale cellular capacity by augmenting coverage regions of macro base stations with lower powered "small cells" [11, 15, 44]. These small cells can be deployed in locations where the macro cell provides poor coverage due to increased distance or obstacles such as high buildings. A macro-cell region (with coverage radius of 1-25Kms) can be expected to support 1-10 small cells [6] (each with coverage radius spanning 0.1-1Kms) [1, 13, 39, 40]. Recent years have witnessed a sharp increase in such multi-cell deployments. At the end of 2022, there were 142K macro-cell towers across the US, and a total of 452K outdoor small cell nodes [8]. It is projected

that by 2027, there will be 13 million outdoor 5G small cell deployments at a global level [7].

One way to deploy multiple cells is to partition the frequency bandwidth among cells, such that they never interfere on the same band. However, such static partitioning of frequency can result in severe under-utilization of the network and reduced user throughput (as highlighted in Appendix A). Therefore, an increasingly common mode of deploying multiple cells is for all the cells to share the same frequency band, which avoids partitioning the bandwidth, thereby increasing the overall network capacity [20, 22]. This, however, results in interference, and necessitates a mechanism for managing it.

## 2.4 Interference Management

Interference management has been studied in 4G context (without slicing). CoMP (Coordinated Multi-Point) [5, 29, 36, 37, 40, 51] encompasses a suite of techniques for managing interference that vary in their deployment complexity. These include techniques such as coordinated beam-forming, coordinated muting, etc. In this paper, we focus on coordinated muting, which enables *muting* selected RBGs on selected cells during each TTI to manage interference.

When compared to other CoMP strategies, muting is far more feasible to implement. It requires the cells to synchronize and coordinate with one another at per-TTI timescales of $\approx 100s\ \mu s$. Prior work demonstrated the feasibility of deploying muting [29, 30], and of achieving sub-ms coordination between cells [40]. More recently, the move towards virtualized RAN, where RAN processing is deployed in servers hosted in the edge datacenters (away from, but still in the geographical vicinity of, the base station) further provides a ready-made platform where such coordinated decisions across multiple cells can take place [35, 55], that can be leveraged by our system.

However, interference management (and muting) has only been explored in the context of optimizing a single objective (i.e. proportional fairness) across all users [10, 27, 45] – we provide a primer on how muting works in this traditional single objective scenario in §3.2. The focus of our work is to manage interference via muting in the presence of RAN slicing, with each slice optimizing its own diverse objective.

## 2.5 Interference Management with Slicing

Summarizing the context so far, prior work on RAN slicing has not considered the problem of interference management in multi-cell scenarios. On the other hand, the prior work on interference management has not considered the new regime of network slicing where users are grouped into slices with diverse objectives.

One exception, that considers both interference management and slicing, is RSEP [21]. RSEP proposes an extreme

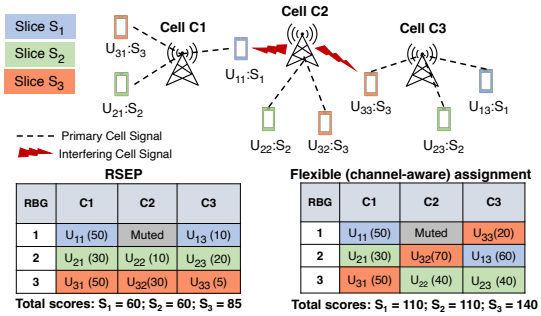


| RBG | C1 | C2 | C3 |
|---|---|---|---|
| 1 | $U_{11}$ (50) | Muted | $U_{13}$ (10) |
| 2 | $U_{21}$ (30) | $U_{22}$ (10) | $U_{23}$ (20) |
| 3 | $U_{31}$ (50) | $U_{32}$(30) | $U_{33}$ (5) |

| RBG | C1 | C2 | C3 |
|---|---|---|---|
| 1 | $U_{11}$ (50) | Muted | $U_{33}$(20) |
| 2 | $U_{21}$ (30) | $U_{32}$(70) | $U_{13}$ (60) |
| 3 | $U_{31}$ (50) | $U_{22}$ (40) | $U_{23}$ (40) |

**Figure 3:** Three RBGs at three cells assigned across users split among three slices. The numbers in paranthesis denote the datarate achieved by the scheduled user. RSEP (left) restricts slices to use the same RBGs across cells. A more flexible channel-aware assignment (right) results in higher performance across all slices.

solution of assigning a given slice exactly the same set of resource block groups (RBGs) at each cell. We depict this in Fig. 3 with the table on the left – slice $S_1$ is assigned the first RBG at each of the three cells ($C_1$, $C_2$ and $C_3$), while slices $S_2$ and $S_3$ are assigned the second and third RBG respectively at each cell. Such an assignment ensures that any muting decision for an RBG only affects users from the same slice at the neighboring cells. It thereby reduces the problem of muting to the no slicing (single objective) setting. However, such a constrained assignment inherently ignores channel diversity, where the channel quality on a given RBG varies drastically depending on which user is scheduled on it [17, 18, 53] (as explained in §2.1). This results in inefficient usage of the radio spectrum and reduced network throughput (up to 40% lower than channel-aware slicing [18]).

Fig.3 illustrates this through a simple example. The table on the left shows the schedule with RSEP, where each slice is restricted to use the same RBG at each cell. Slice $S_1$ prefers to mute its assigned RBG at cell $C_2$ to boost the channel quality of its user $U_{11}$ at the neighboring cell $C_1$. Slice $S_1$'s user at $C_3$ ($U_{13}$) is not significantly impacted by interference from $C_2$. The numbers in paranthesis denote the datarate (throughput) achieved by the scheduled user. The total datarate experienced by Slices $S_1$, $S_2$, and $S_3$ (summed across their scheduled users) is 60, 60, and 85 respectively.

The table on the right shows a more "flexible" assignment of RBGs across slices that can leverage channel diversity. Such an assignment can achieve superior performance by allowing different slices to use different RBGs across different cells, as per their respective channel qualities (e.g. RBG 2 is assigned to slice $S_2$ at cell $C_1$ and to slice $S_3$ at cell $C_2$). The unrestricted assignment further allows a given muting decision to simultaneously benefit multiple slices thus amortizing the cost of muting (for e.g. muting the transmission of RBG 1 at cell $C_2$ boosts the channel qualities of users $U_{11}$ and $U_{33}$ in Slice $S_1$ and Slice $S_3$ respectively). In this case,

the total datarate, summed across all scheduled users for Slices $S_1$, $S_2$, and $S_3$ is 110, 110, and 140 respectively; which is higher across the board when compared to RSEP.

While this is a toy example, our evaluation with real-world traces in §6 reinforces the performance benefits of such "flexible" channel-aware assignment of RBGs across slices and cells, when compared to RSEP's restricted assignment.

However, enabling such flexible channel-aware assignment requires reasoning about the muting decision across multiple slices with diverse objectives: Is it okay to mute the first RBG at $C_2$ to benefit slices $S_1$ and $S_3$? Which slice incurs the cost of this muted RBG and how? We need a way to answer such questions in a manner that still retains performance isolation across slices. Our system, SiRAN, deals with this challenge.

## 3 Primer on Relevant Mechanisms

Before diving into SiRAN's design, we provide a brief primer on mechanisms for channel-aware slicing at a single cell (§3.1), and for interference mechanism via muting in a no slicing setting with a single global objective (§3.2).

### 3.1 Channel-aware Slicing and Scheduling

**Channel-Aware Inter-Slice Scheduling.** SiRAN leverages RadioSaber [18] for channel-aware slicing at each cell, where an *inter-slice* scheduler assigns RBGs to slices and an *intra-slice* scheduler assigns RBGs to users within the slice. In each TTI, the *inter-slice* scheduler greedily assigns RBGs to slices, one RBG at a time as follows. It queries each *intra-slice* scheduler asking which user will be scheduled on the RBG if that RBG is assigned to that slice. Each slice responds to this query based on its own intra-slice scheduling policy (detailed next). The responses allow the *inter-slice* scheduler to determine the channel quality associated with that RBG for each slice (based on which user each slice picks). It then assigns the RBG to the slice with the highest channel quality. As mentioned in §2.2, each slice has a per-TTI quota of RBGs derived from its SLA. While greedily assigning RBGs to slices, the scheduler tracks their quota, and avoids assigning more RBGs to slices that have exhausted their quotas.

**Channel-Aware Intra-Slice Scheduling.** For a given RBG $R_i$, the *intra-slice scheduler* assigns each of the slice's user $u_k$ a score ($score(u_k, R_i)$) based on the desired performance objective of the slice. It then assigns $R_i$ to the user with the highest score. For example, a slice wanting to maximize throughput would set $score(u_k, R_i) = inst\_rate(u_k, R_i)$ (i.e. the instantaneous data rate $u_k$ would achieve if it is allocated $R_i$, as per its channel quality for $R_i$). A slice can optimize for proportional fairness (a popular objective in cellular networks [28, 34, 53]) by weighing the instantaneous rate with the average rate allocated to $u_k$ so far, i.e. by setting $score(u_k, R_i) = \frac{inst\_rate(u_k, R_i)}{avg\_rate(u_k)}$. The scores can also be weighed as per user priorities. Such score-based scheduling of RBGs across users is also adopted in a no slicing setting, where all users share a common global objective [17].

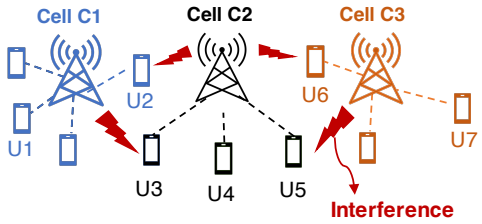


| Muting Hypothesis | C1 | C2 | C3 | Overall Score |
|---|---|---|---|---|
| H0: No muting | U1 (10) | U4 (15) | U7 (30) | 55 |
| H1: Mute C1 | Muted | U3 (40) | U7 (30) | 70 |
| H2: Mute C2 | U2 (50) | Muted | U6 (60) | 110 |
| H3: Mute C3 | U1 (10) | U5 (20) | Muted | 30 |

**Figure 4:** Example showing muting for a single objective (no slicing). The figure shows user locations with respect to cells. The table on the bottom shows the assignment of RBG $R_i$ at each cell for the different muting hypotheses. The number in parentheses indicates the score for the corresponding user. Muting RBG $R_i$ at cells $C_1$ or $C_2$ produces a net benefit, while muting it at $C_3$ produces a net loss.

### 3.2 Muting under a Single Objective

We next detail how muting decisions are made without slicing where all users share a single global objective. Past work adopts a greedy strategy for this [10, 27, 45]. In each TTI, we greedily pick RBG $R_i$, and analyze the cost-benefit trade-off of muting that RBG at each cell, one cell at a time (referred to as the muting hypothesis). It is beneficial to mute $R_i$ at cell $C_j$ if the boost in channel quality at the neighboring cells overpowers the penalty of losing out on that RBG at $C_j$. To assess this, we compute the system-wide total score under each muting hypothesis $H_j$ (where $R_i$ is muted at cell $C_j$) and under no muting (denoted as hypothesis $H_0$). The total score under hypothesis $H_j$ is computed as: $\sum_{u_k \in U(R_i, H_j)} score(u_k, R_i)$. Here, $U(R_i, H_j)$ denotes the set of users that are scheduled on $R_i$ at each cell under hypothesis $H_j$. The user scores are computed as described in §3.1, as per the shared global objective.

The difference between the total score of a muting hypothesis $H_j$ and no muting hypothesis $H_0$ gives us the net benefit of muting RBG $R_i$ at cell $C_j$. If the net benefit is negative for all muting hypothesis, $R_i$ is not muted at any cell. Otherwise, we select the hypothesis with the largest net benefit and mute the RBG at that cell.

Fig. 4 presents an example for this, where we have 3 cells and want to determine whether or not to mute the transmission of a cell on a given RBG $R_i$. Hypothesis $H_0$ is when $R_i$ is not muted at any cell (top row in Fig. 4). The three cells

schedule UEs $U_1$, $U_4$ and $U_7$, that do not experience significant interference from other cells. The total score for $H_0$ (last column) is computed by adding the scores of each of these three UEs (indicated in parentheses). The next hypothesis $H_1$ (second row) is where $R_i$ is muted at $C_1$ – this impacts the scheduling decision at cell $C_2$, boosting channel quality of "edge" UE $U_3$. The set of scheduled UEs, based on whom $H_1$'s total score is computed, therefore includes $U_3$ at $C_2$ and $U_7$ at $C_3$. Likewise, hypothesis $H_2$ (third row), where $R_i$ is muted at $C_2$, boosts the channel quality of "edge" UEs $U_2$ and $U_6$, and they get scheduled on this RB at cells $C_1$ and $C_3$ instead. The overall score of $H_2$ is computed by adding their scores. We similarly consider the impact of muting $R_i$ at $C_3$ and compute the overall score of $H_3$.

Comparing scores of $H_1$, $H_2$ and $H_3$ with $H_0$, we can see how muting $R_i$ at $C_1$ or $C_2$ produces a positive net benefit while muting it at $C_3$ incurs a loss. The benefit of muting at $C_2$ is higher, so the system will mute $R_i$ at $C_2$. This freezes the muting and scheduling decision for that RBG, and we then move on to the next RBG and repeat the same steps.

A few points are worth noting:

• In the above example, we could have additional hypotheses where we mute $R_i$ on more than one cell (resulting in $2^M$ hypothesis for each RBG, where $M$ is the number of cells). We observed that muting multiple cells for the same RBG provides limited benefit since most interference occurs between the macro-cell and small cells, i.e., muting either the macro-cell or one of the small cells that interferes with the user being served by the macro-cell is sufficient. So we restrict the assessment to consider muting up to one cell per RBG (making the number of hypotheses linear in $M$).

• The muting hypothesis is evaluated without actually muting the cell – it uses knowledge about the channel quality each user will experience with and without interference from the neighboring cells. (The 3GPP standard specifies the use of specific "resource elements" to enable such interference measurement [9, 19], as detailed in Appendix B).

# 4 SiRAN Design

SiRAN uses the greedy muting approach described in §3.2, where in each TTI, it greedily decides whether or not to mute an RBG at any cell, one RBG at a time. However, rather than catering the muting decision towards a single shared objective across all users, SiRAN makes these decisions in manner that respects individual slice objectives (as described in the remainder of this section). The greedy per-RBG muting decisions are made jointly with greedy channel-aware scheduling decisions (i.e. which users, belonging to which slice, should be scheduled on the unmuted RBGs) – SiRAN uses RadioSaber's scheduling logic for this, as described in §3.1. Jointly making muting decisions with channel-aware

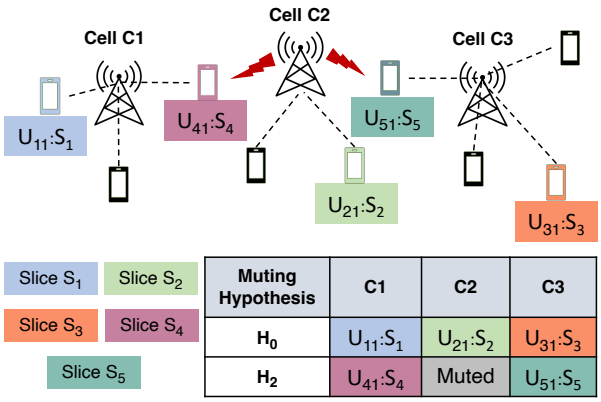


**Figure 5:** The example above shows the assignment of RBG $R_i$ across slices under no muting hypothesis ($H_0$) and the hypothesis where the RBG is muted at cell $C2$ ($H_2$). The numbers in parenthesis indicate the user's slice association.

RAN slicing, requires SiRAN to address multiple challenges, that we detail in this section:

(1) *How do we reason about a muting hypothesis while maintaining performance isolation between slices?* (§4.1)
(2) *How do we efficiently compute the benefit of a muting decision for a given slice based on its own objective?* (§4.2)
(3) *How do we efficiently compute the cost of a muting decision for a given slice based on its own objective?* (§4.3)
(4) *How do we decide which muting hypothesis to implement (i.e. which cell to mute on an RBG) when different slices benefit from different decisions?* (§4.4)

## 4.1 Reasoning about a muting hypothesis

While it is straightforward to reason about muting decisions when all users share a single common objective (as described in §3.2), SiRAN must deal with the challenge of handling diverse slice objectives in a manner that maintains performance isolation between slices. Fig. 5 illustrates the challenge by considering how an RBG $R_i$ is assigned to users across slices under no muting and when it is muted at cell $C_2$. When $R_i$ is not muted (hypothesis $H_0$, top row), users of slices $S_1$, $S_2$ and $S_3$ are scheduled on $R_i$ at cells $C_1$, $C_2$ and $C_3$, respectively. Muting $R_i$ at $C_2$ (hypothesis $H_2$, bottom row) changes the channel quality (and scores) of users in the neighboring cells $C_1$ and $C_3$, causing $R_i$ to be assigned to a different set of slices ($S_4$ at $C_1$ and $S_5$ at $C_3$). It therefore appears as if the decision to mute RBG $R_i$ at cell $C_2$ benefits slices $S_4$ and $S_5$, at the cost of slices $S_1$, $S_2$, and $S_3$. How do we make a systematic choice in such a scenario – is it okay to help some slices at the cost of others? Wouldn't that violate performance isolation across slices? SiRAN effectively *avoids* making such choices using the following insight:

**Resource attribution to retain isolation.** Rather than considering a muted RBG at a cell $C_j$ as a wasted resource that belongs to no one, we count it towards the quota of

the $K$ slices that benefit from muting it, i.e. we reduce the quota of those slices at $C_j$ by $1/K$ RBGs. This restricts the cost of muting (i.e., reduction in available resources at $C_j$) to these $K$ slices that benefit from boosted channel qualities at neighboring cells. This, in turn, enables independent cost-benefit analysis based on the specific objectives of these slices.

Revisiting the example in Fig. 5: given how we account for the muted resource, since the quotas of $S_1$, $S_2$, and $S_3$ remain intact, they are not really penalized by the decision to mute $R_i$ at $C_2$ – each of these slices would simply be assigned a different RBG at cells $C_1$, $C_2$, and $C_3$ respectively. $S_4$ and $S_5$, in contrast, may lose some quota at $C_2$ if the RBG is muted – the cost of losing that quota at $C_2$ should be compared with the benefit that these slices experience at cells $C_1$ and $C_3$ due to muting. For instance, if serving $S_4$'s user $U_{41}$ at $C_1$, comes at the cost of penalizing a higher priority user at $C_2$ due to the reduced quota, $S_4$ might not want to proceed with the muting decision.

**Challenge.** How do we identify the set of $K$ slices that benefit from muting, if weighing the benefit vs. the cost of muting depends on $K$ itself (as we reduce the quota of benefiting slices by $1/K$ RBGs)?

**Our approach.** We use an iterative algorithm (summarized in Fig. 6). Consider the hypothesis $H_j$ of muting $R_i$ at $C_j$:

**(i)** We start with assuming that each slice that uses $R_i$ at $C_j$'s neighboring cells (i.e. at $C_n \neq C_j$) under $H_j$ is benefited by the muting. We refer to this set of slices as $\mathcal{S}$. We accordingly reduce the quota of each slice in $\mathcal{S}$ by $\frac{1}{|\mathcal{S}|}$ RBGs at cell $C_j$.

**(ii)** We then individually assess the benefit (§4.2) and cost (§4.3) of muting for each slice in $\mathcal{S}$. If the assessment reveals a slice $S'$ in $\mathcal{S}$ is hurt by muting (i.e. the cost it pays due to the quota reduction at $C_j$ is higher than the benefit it gets at the neighboring cells), then we exclude it from participating in the muting decision. Specifically, we undo the reduction in quota of slice $S'$ at $C_j$, and remove it from the set $\mathcal{S}$. This reduces the size of set $\mathcal{S}$, thereby increasing the share of quota reduction at $C_j$ for the remaining slices in $\mathcal{S}$.

**(iii)** We accordingly update the cost of muting for the remaining slices in $\mathcal{S}$, and re-assess the benefit vs cost of muting for each of these slices as per step (ii).

**(iv)** We repeat steps (ii) and (iii) in a loop until the set $\mathcal{S}$ stops changing, giving us the converged set of $K = |\mathcal{S}|$ slices that benefit from the muting hypothesis. (The number of iterations is bounded by the number of cells.)

So for our example in Fig. 5, we will start by assuming both $S_4$ and $S_5$ benefit from muting hypothesis $H_2$, and evaluate the cost of reducing 0.5×RBG from the quota of both of these slices at $C_2$. If the cost of muting for $S_4$ turns out to be higher than the benefit it sees, $S_4$ will get back its quota of 0.5×RBG at $C_2$ and it will be removed from $\mathcal{S}$. The muting hypothesis $H_2$ will then be considered valid if $S_5$ sees sufficiently high benefit over the cost of 1×RBG quota reduction at $C_2$.

The following is worth noting.

• **Slice eligibility for muting.** A slice in $\mathcal{S}$ can participate in the muting decision only if it has sufficient quota (at least $\frac{1}{|\mathcal{S}|}$ RBGs) remaining at $C_j$ to pay for the cost of muting. If a slice has exhausted all of its quota at $C_j$ (from the previously allocated RBGs in that TTI), then it cannot induce muting at $C_j$ and cannot be added to the set $\mathcal{S}$.

• **Valid muting hypothesis.** We consider $H_j$ to be a valid hypothesis if the resulting set $\mathcal{S}$ is non-empty (i.e. there are non-zero number of slices that benefit from the muting decision after paying the shared cost of muting). We similarly check the validity of other muting hypothesis (i.e. of muting $R_i$ at other cells). If none of the muting hypotheses for $R_i$ are valid, we do not mute it at any cell. If there are multiple valid muting hypotheses, we select one (as detailed in §4.4) and proceed with that decision.

## 4.2 Computing Benefit of Muting

We now explain how SiRAN computes the benefit of a given muting hypothesis for a given slice in $\mathcal{S}$. Let us refer again to the example in Fig. 5, and consider how to compute the benefit of muting hypothesis $H_2$ (i.e muting of RBG $R_i$ at $C_2$) that slice $S_4$ enjoys at the neighboring cell $C_1$. At a high-level, this can be computed by comparing the score of $S_4$ at cell $C_1$ with and without muting $R_i$ at $C_2$ (with scores defined based on the slice's objective, as detailed in §3.1). However, naively comparing the assignment of $R_i$ under $H_2$ with the no muting hypothesis $H_0$, it would seem that the performance of $S_4$ (which was not even assigned $R_i$ at any cell under $H_0$) is far better under $H_2$ (where it is assigned $R_i$ at $C_1$). This is a misleading assessment that overestimates the benefit of muting. This is because, by getting scheduled on $R_i$ at $C_1$ under hypothesis $H_2$, $S_4$ uses up a quota of 1 RBG at $C_1$. It will therefore be scheduled on 1 less RBG among the remaining $N-1$ RBGs in that TTI under $H_2$, when compared to the remaining $N-1$ RBGs under $H_0$.

In order to truly assess the benefit of muting, we need to compare how the RBG quota used by $S_4$ to schedule user $U_{41}$ on $R_i$ under $H_2$ compares to the use of that RBG quota under $H_0$. This ideally requires comparing the total score of $S_4$ across hypotheses $H_0$ and $H_2$, not just for RBG $R_i$, but for all of the remaining $N-1$ RBGs in that TTI, such that we can account for how that RBG quota is subsequently used under $H_0$. This implies that we need to run the scheduler to compute the hypothetical assignment of UEs on these remaining $N-1$ RBGs for each muting hypothesis that we wish to greedily assess for each RBG. As we show in §6, the $O(N^2)$ complexity induced by this is prohibitively expensive, given the tight TTI timescales at which scheduling and muting decisions must be made. So how do we work around this?

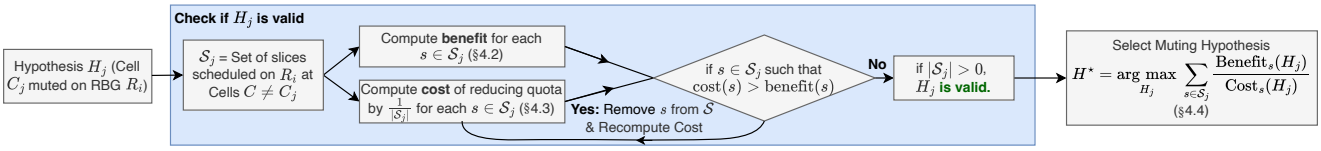


**Figure 6:** SiRAN's Workflow

**Our approximation technique.** We use a simple heuristic to *approximate* the benefit of muting without re-running the scheduler for the remaining RBGs. Referring to our example in Fig. 5, in order to assess the benefit to $S_4$ at neighboring cell $C_1$ under hypothesis $H_2$, we compute which $S_4$ user would have hypothetically been allocated $R_i$ at $C_1$ under no muting, if that RBG was restricted to being allocated exclusively to $S_4$. We then subtract $S_4$'s score at $C_1$ obtained from this hypothetical assignment of $R_i$ under no muting from its score at $C_1$ under hypothesis $H_2$. We use the outcome as our proxy for the benefit of muting. This essentially captures the impact of reducing interference from $C_2$ for slice $S_4$'s users at $C_1$.

However, it masks the impact of channel diversity in our assessment (since in reality, $S_4$ is not allocated $R_i$ under no muting, but would instead be allocated a different RBG). Nonetheless, we find this approximation works well in practice because in situations where the benefit substantially outweighs the cost of muting, the effect of interference mitigation overpowers the effects of channel diversity. When the benefit is low (interference effects are small), the slice is anyway removed from set $\mathcal{S}$, and the precise value of the benefit does not make a difference.

If a given slice $S_k$ has users scheduled in $R_i$ at multiple neighboring cells under hypothesis $H_j$, we approximate the benefit seen by $S_k$ at each of these cells and sum them up to get the overall benefit to $S_k$ for hypothesis $H_j$.

## 4.3 Computing Cost of Muting

As mentioned before, we account for the cost of muting RBG $R_i$ at $C_j$ by subtracting $\frac{1}{|\mathcal{S}|}$RBGs at cell $C_j$ from the quota of each slice in set $\mathcal{S}$ (that benefit from the muting). Assessing this cost for a given slice $S_k$ requires comparing how $S_k$ is scheduled on remaining RBGs at $C_j$ with and without muting (i.e. with and without the quota reduction). This causes two hurdles. First, as discussed in §4.2, re-running the schedulers across all remaining RBGs for each muting hypothesis is prohibitively expensive. Second, how do we even assess the impact of fractional quota reductions? RBGs must be wholly allocated to a single user, and cannot be split across multiple users. When multiple slices have non-integral quotas, the scheduler allocates the last RBG in the TTI (that must ideally have been split between these slices) to one of these slices picked randomly. It then keeps track of the (fractional) surplus or deficit in quota allocation, that rolls over to the next TTI. Rolling over of fractional offsets ensures that a slices pays its due cost of muting over time. But the impact of that might not be seen in that TTI, and re-running the scheduler over multiple TTIs would increase the computational complexity further.

**Our approximation technique.** At the start of each TTI, we run the scheduler once to determine an initial assignment of each RBG under the hypothetical scenario where no RBG is muted at any cell. We use this as a reference schedule to assess how much an RBG is worth to a given slice at a given cell and accordingly compute the cost of quota reduction, when assessing individual muting hypothesis for each RBG (without re-running the scheduler).

The worth of an RBG for $S_k$ at cell $C_j$ increases as we keep reducing the slice's quota at that cell. This is because when a slice's quota is reduced, it will kick out (i.e. avoid scheduling) users on RBGs with the lowest score. Further quota reduction incurs a higher cost, by kicking out users with higher scores. We account for this by clustering RBGs based on their scores and using the average score within each cluster as the worth of the RBG in that cluster. (We use a cheap clustering logic based on standard deviations from the average score.) When computing the cost of quota reduction, we first consider RBGs in the lowest score cluster. If the average score of that cluster is $X$, then a quota reduction of 0.5 has a cost of $0.5X$. If the total quota reduction for a slice (summed across muting decisions over multiple RBGs) exceeds the number of RBGs in the lowest score cluster, we move over to the next lowest score cluster, and so on.

The reference schedule does not account for potential muting at other cells which can increase the worth of RBGs. Therefore, the cluser average scores taken directly from the reference schedule as described above can underestimate the cost that slice $S_k$ incurs for muting at $C_j$. To compensate for that, we update $S_k$'s average score for each RBG cluster at $C_j$ by multiplying it with an error ratio $\beta$. We compute $\beta$ from past observation – by how much did $S_k$'s estimated score at $C_j$ in the previous TTI $t$ differed from the actual score it achieved at $C_j$ in that TTI. Specifically, $\beta = \frac{A_{j,k,t}}{E_{j,k,t}}$, where $A_{j,k,t}$ is the (actual) average score across all RBGs actually assigned to $S_k$ at $C_j$ in TTI $t$ and $E_{j,k,t}$ is the (estimated) average score across all RBGs assigned to $S_k$ at $C_j$ in the reference schedule during the previous TTI $t$.

## 4.4 Comparing Muting Hypotheses

We use the benefit and cost computed as described above to assess whether the muting hypothesis is valid as outlined in §4.1. We empirically observed that in most cases, at most one muting hypothesis is valid for a given RBG (for the reason explained in §3.2). When there are multiple valid muting hypothesis $H_j$, we pick one as follows. For each valid muting hypothesis $H_j$, we compute the total benefit seen by each slice in set $\mathcal{S}_j$ (where set $\mathcal{S}_j$ is the converged set of benefiting slices in $H_j$) and divide it by the cost incurred by that slice. We then sum this benefit to cost ratio across all slices in set $\mathcal{S}_j$, and favor the muting hypothesis that has the highest value for this sum.

# 5 Implementation

**Customizing Slice Objectives.** We leverage the interface provided by RadioSaber [18] to enable slice operators to customize their objectives using certain parameters. In particular, for a given slice $S_k$, we assign the following score to user $u_m$ in the slice for RBG $R_i$: $score(u_m, R_i) = w_m \times \frac{inst\_rate(u_m,R_i)}{(avg\_rate(u_m))^\alpha}$, where $w_m$ is the weight of user $u_m$ (set based on its relative priority) and $\alpha \in \mathbb{R}_{\geq 0}$ controls the degree of fairness. This directly maps to optimizing a well known parameterized objective known as weighted alpha-fairness [31] for that slice. Each slice can configure $w_m$ and $\alpha$ differently to capture different objectives. With equal weights across all users, setting $\alpha = 0$ maximizes throughput (MT). Setting $\alpha = 1$ achieves proportional fairness (PF), where the $\alpha$-fair objective is reduced to maximizing $\sum_{u_m \in U_k} w_m log(x_m)$ (where $x_m$ is the throughput achieved by $u_m$). Increasing $\alpha$ further increases the degree of fairness among users of the slice in terms achieved throughput.

**Implementation in Simulator.** Due to the absence of required features in current versions of open-source RAN testbeds (notably, per-RBG muting capability), we evaluate our system using trace-driven simulations that further allows us to scale to hundreds of users. We implement SiRAN in an open-source cellular simulator [18, 43]. Our simulator configuration for 5G small cell deployment (detailed in §6) adheres to the 3GPP-specified parameters [6].

**Collecting user traces.** We use NG-Scope [54] deployed on USRP X310 to collect real-world channel quality data from cellular base-stations across different frequency bands and operators. The tool allows us to extract fine-grained metrics that capture channel quality of the UE across different RBGs over time. We move around with this setup to collect channel quality traces at different locations relative to the transmitting cell, mapping different chunks of the resulting trace to different users in our simulations.

**Software Implementation.** We also implement SiRAN as a separate module in software on a 12th Gen Intel Core i9-12900F machine in order to evaluate its computational overhead. Specifically, we assess the time it takes for making its joint scheduling and muting decisions across all RBGs in a TTI for different 5G configurations (that vary in TTI duration and the number of RBGs per TTI). Our software implementation aligns with the move towards virtualized RAN, where RAN processing is done in software [3, 55].

# 6 Evaluation

Our evaluation is divided into three key components:

**1. Comparison with Baselines.** In §6.2, we use trace-driven simulations across scenarios spanning hundreds of users split across slices with diverse objectives to show how SiRAN consistently outperforms the following baselines:

*(i) RadioSaber [18]:* that does channel-aware slicing at each cell without any interference management.

*(ii) Single objective muting (SOM [10, 27, 45]):* This baseline uses channel-aware RAN slicing, and schedules RBGs across users within each slice as per their individual objectives. However, it uses the single objective muting algorithm discussed in §3.2 to assess the scores of scheduled users and make its muting decision as per the specified global objective agnostic of individual slice objectives.

*(iii) RSEP [21]:* that assigns a given slice the same set of RBGs at each cell, thereby ignoring channel diversity when scheduling RBGs. It then performs objective-based muting decisions for individual slices in isolation.

**2. Comparison with Exhaustive Approach.** In §6.3, we evaluate how SiRAN's techniques to approximate the benefit and cost of muting closely match the outcome of the more rigorous (exhaustive) assessment that requires repeatedly rerunning the scheduler. SiRAN's logic comfortably fits within the TTI budget across different 5G configurations, while the exhaustive approach is prohibitively expensive.

**3. Factor Analysis.** We individually evaluate the impact of certain design choices made by SiRAN in Appendix E.4.

## 6.1 Experiment Settings

We simulate a multi-cell deployment comprising one macro cell and four small cells (similar to what is depicted in Fig. 2) [6, 40]. We configure each cell with a bandwidth of 100 MHz, split across 512 RBs per TTI, grouped into 64 RBGs [49]. The small cells are deployed uniformly within the macro-cell's coverage region at a randomly-chosen distance of at least 300m from the macro-cell and 500m from neighboring small cells. We simulate 160 users split across 8 slices [6]. We situate each user within the coverage region of a randomly selected small cell with a probability of 2/3, and outside of the coverage region of any small cell (thereby attached to the macro-cell) with probability 1/3. Of the total users, 60% are static while 40% are mobile (traveling at speeds ranging from 3 to 30 km/h). Once a user is generated, we apply the 3GPP

| Parameter | PF Slices | TP Slices |
|---|---|---|
| # Slices | 4 | 4 |
| Traffic Pattern | Backlogged | Backlogged |
| Objective | PF | Max Throughput |
| Metric | $\sum_i \log x_i$ | avg tpt |
| Result | Fig. 7b | Fig. 7c |

**(a)** Scenario 1 configuration

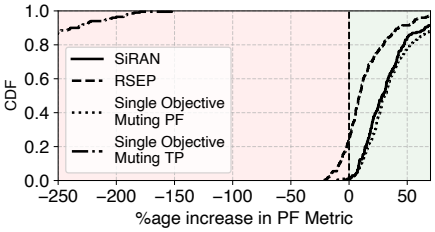


**(b)** Per slice performance of PF slices

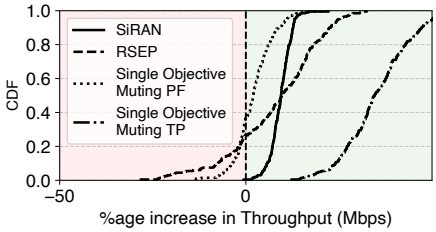


**(c)** Per slice performance of MT slices

**Figure 7:** SiRAN's, RSEP's and SOM-PF's and SOM-TP's impact on slice-level performance when compared to RadioSaber (no muting) for (b) PF slices and (c) Max TP slices under Scenario 1, aggregated across 50 experiment runs with different seeds.

urban area path loss model to calculate the user's wideband channel quality (aggregated across all RBGs) based on its distance from each cell. We then assign a real-world trace to each user that maps the computed wideband value for each cell (thereby extracting the effects of channel diversity from real-world conditions). We use the standard policy of assigning each user the serving cell from which it experiences highest wideband channel quality. We configure each slice to have the same quota of RBGs at each cell.

We vary the slice objectives and user traffic patterns across different scenarios, and test the scenarios against different scheduling and muting schemes described above. For each setting, we run experiments with multiple random seeds that end up varying the specific user locations, and user distribution across cells and slices. We capture different slice objectives by varying the parameters of weighted $\alpha$-fairness (as described in §5). We experiment with two categories of user traffic patterns: (i) backlogged (representing high bandwidth video streaming, gaming, etc that would saturate the datarate allocated to the user), and (ii) web flows (fixed sized flows with Poisson inter-arrival times and flow sizes drawn from a heavy-tailed distribution [41], generated at an average rate of 10Mbps).

## 6.2 Comparative Evaluation

We use RadioSaber without muting as the reference baseline and report the relative changes induced by SiRAN, SOM, and RSEP over it for the given slice-objective.

**Scenario 1: proportional fairness and maximizing throughput.** In our first scenario (summarized in Table 7a), we configure four slices with proportional fair (PF) objective by setting $\alpha = 1$. We refer to these as "PF slices". The remaining four slices (referred to as MT slices) are configured with the objective of maximizing throughput (MT) by setting $\alpha = 0$. We accordingly experiment with two different variants of SOM baseline, one configured with PF as the global objective and another with MT as the global objective. Fig. 7 reports the results (aggregated over 50 runs): In Fig 7b we compute the percentage improvement in the PF metric for each of the PF slices, when compared to RadioSaber (no muting), and plot the resulting CDF. Fig 7c similarly plots the CDF of the percentage improvement in the total throughput over RadioSaber (no muting) for each of the MT slices.

*(i) SiRAN vs RadioSaber without muting:* SiRAN's interference management benefits slices across the board when compared to no muting, resulting in an average of 33.5% increase in PF metric for the PF slices (Fig 7b) and 9.3% increase in throughput for the MT slices (Fig7c).

*(ii) SiRAN vs SOM:* SOM's performance depends on how the global objective is configured. SOM-PF (configured with PF objective) results in an average of 37.4% increase in PF metric over RadioSaber without muting (similar to SiRAN) for the PF slices. However, it comes at the cost of hurting a large proportion of MT slices (more than 37% slices, as shown in Fig. 7c) whose objective does not align with SOM-PF, hence violating performance isolation. In contrast, SOM-MT (configured with MT objective) substantially improves throughput for the MT slices (with an average increase of 35.2% over no muting), but it comes at the cost of significantly hurting the PF slices thereby violating performance isolation between slices (we cut off the x-axis at -200%, so the extent of this cost is not fully visible). This drastic penalty is caused by the gross misalignment between SOM's muting objective (MT) and the slice's scheduling objective (PF), where the PF slice often allocates RBGs to relatively poor users (that suffer from low channel quality) in order to achieve fairness, and SOM optimizing for throughput pointedly mutes those RBGs (with low MT scores), thereby degrading the PF metric.

*(iii) SiRAN vs RSEP:* RSEP's performance is inferior to SiRAN's across all PF slices, with 18.4% lower PF metric than SiRAN on an average. For the MT slices, RSEP fares slightly better than SiRAN for half of the slices (which are incidentally allocated reasonably good RBGs and benefit from isolated muting decisions with RSEP). However, it has worse throughput than SiRAN for the other half, of which 26.5% slices have even worse throughput than the baseline, caused by RSEP's channel-unaware scheduling.

**Scenario 2: varying degree of fairness.** In this scenario (summarized in Table 8a), we configure four slices (referred as PF slices) with proportional fair (PF) objective by setting

| Parameter | PF Slices | $\alpha = 3$ Fair Slices |
|---|---|---|
| # Slices | 4 | 4 |
| Traffic Pattern | Backlogged | Backlogged |
| Objective | PF ($\alpha = 1$) | Fairness with $\alpha = 3$ |
| Metric | $\sum_i \log x_i$ | 10%ile, avg tpt |
| Result | Fig. 8b | Fig. 8c Fig. 8d |

**(a)** Scenario 2 configuration

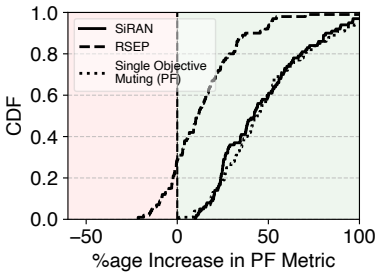


**(b)** Per slice performance of PF-slices

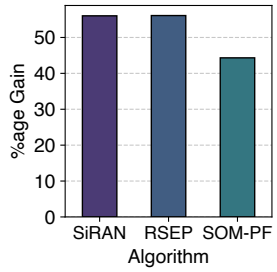


**(c)** % increase in 10$^{th}$ percentile throughput across users in $\alpha = 3$

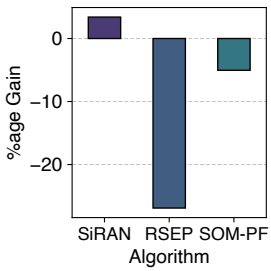


**(d)** % increase in avg throughput across users in $\alpha = 3$ Fair slices

**Figure 8:** SiRAN's, RSEP's and SOM's impact on slice-level performance when compared to RadioSaber (no muting) for the (b) PF slices and (c, d) $\alpha = 3$ Fair slices under Scenario 2, aggregated across 50 experiment runs with different seeds.

$\alpha = 1$. The remaining four slices were configured with an objective with higher degree of throughput fairness ($\alpha$ set to 3). We refer to these as "$\alpha = 3$ Fair slices". We configure the SOM baseline with a global objective that maps to PF. All users are configured with backlogged traffic pattern. We report the results (aggregated over 50 runs with different seeds) in Fig 8. Fig 8b plots the CDF of percentage improvement in the PF metric experienced by each of the PF slices, when compared to RadioSaber (no muting). Fig. 8c plots the percentage improvement in the throughput of the poorest (lowest 10%ile) users over RadioSaber (no muting), as a measure of fairness for $\alpha = 3$ Fair slices. Fig. 8d plots the corresponding percentage improvement in the average throughput across all users for $\alpha = 3$ Fair slices. We have the following key takeaways:
*(i) SiRAN vs RadioSaber without muting:* SiRAN's interference management benefits slices across the board. For the set of PF slices, the corresponding PF metric of each slice increases with muting (as shown in Fig 8b), resulting in 48.0% average improvement over RadioSaber without muting. For the set of $\alpha = 3$ Fair slices, the throughput of the poorest (lowest 10%ile users) increases by 56.1% with SiRAN (Fig. 8c). The average throughput (not directly aligned with fairness objective) also improves by a marginal 3.4% (Fig. 8d).
*(ii) SiRAN vs SOM:* We find that SOM, configured with global PF objective, performs as well as SiRAN for the PF slices (Fig 8b). It also improves 10%ile throughput for the $\alpha = 3$ Fair slices by 44.3% over no muting – SOM optimizing for proportional fairness with $\alpha = 1$ helps these users, but not to the same extent as SiRAN that can better tailor its muting decisions with the $\alpha = 3$ fair objective of these slices (Fig. 8c).
*(iii) SiRAN vs RSEP:* RSEP's performance is inferior to SiRAN's across all PF slices, with 33% lower PF metric than SiRAN on an average (Fig 8b). When compared to RadioSaber no mute, RSEP is able to improve performance for 71% of slices due to muting, but 29% slices experience *worse* performance due to channel unawareness. For the $\alpha = 3$ Fair slices, we find that RSEP is able to achieve sufficiently good throughput (similar to SiRAN) for the poorest 10%ile users that are more prone to the effects of interference than channel diversity (Fig. 8c). However, it induces a 26.9% reduction in the average throughput across all users in this category of slices due to channel-unaware scheduling, when compared to RadioSaber, resulting in an overall poorer outcome than SiRAN (Fig. 8d).

**Scenario 3: varying weights across users.** In this scenario (summarized in Table 9a), we configure the first four slices (referred to as WPF slices) with weighted proportional fairness objective, setting $\alpha = 1$, with 40% of randomly selected users having a very high weight of 1000 and web flow traffic pattern, and the remaining 60% users have a weight of 1 and backlogged traffic pattern. The remaining four slices (referred to as PF slices) are configured with proportional fairness objective with equal weight and backlogged traffic pattern across all users. We try two variants of SOM here – SOM-WPF and SOM-PF. SOM-WPF is configured with weighted PF as the global objective (where the prioritized 40% users of WPF slices have a weight of 1000 and all other users have a weight of 1). SOM-PF is configured with PF objective. We report the results in Fig. 9. We consider two metrics for WPF slices: reduction in median flow completion time (FCT) of the prioritized 40% users, when compared to RadioSaber without muting (Fig. 9b), and the average throughput of the remaining 60% users (Fig. 9c). For the PF slices, we report improvement in PF metric over RadioSaber without muting (Fig. 9d), similar to other scenarios.
*(i) SiRAN vs RadioSaber without muting:* SiRAN results in 66.2% reduction in median FCT for the prioritized users in WPF slices over RadioSaber without muting (Fig. 9b), along with a 15.0% improvement in overall throughput of the non-prioritized users (Fig. 9c). Among the PF slices, SiRAN increases the PF metric of all slices (Fig. 9d), with an average increase of 45.1% over no muting.
*(ii) SiRAN vs SOM:* SOM's performance again depends on how the global objective aligns. SOM-WPF results in 68% reduction in median FCT of the prioritized users in the WPF

| Parameter | WPF Slices | PF Slices |
|---|---|---|
| # Slices | 4 | 4 |
| Traffic Pattern | •40% Web Flow ($W$ = 1000x)<br>•60% Back-logged | Backlogged |
| Objective | Weighted PF | PF |
| Metric | Median FCT | $\sum_i \log x_i$ |
| Result | Fig. 9b<br>Fig. 9c | Fig. 9d |

**(a)** Scenario 3 configuration

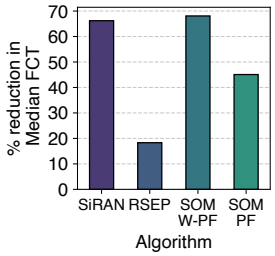


**(b)** Improvement in Median FCT of prioritized web flows

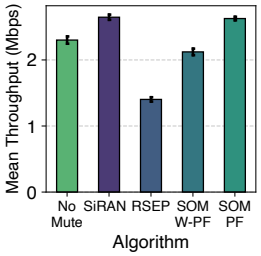


**(c)** Avg throughput of non prioritized flows

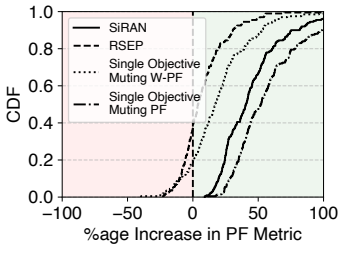


**(d)** Per slice performance of PF slices

**Figure 9:** SiRAN's, RSEP's and SOM W-PF's and SOM-PF's impact on slice-level performance when compared to RadioSaber (no muting) for (b,c) Weighted PF slices and (d) PF slices under Scenario 3, aggregated across 50 experiment runs with different seeds.

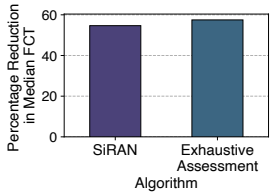


**(a)** Reduction in Median FCT

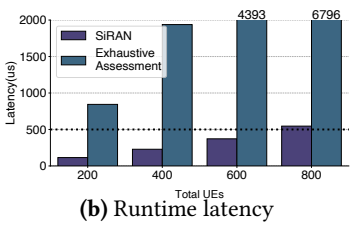


**(b)** Runtime latency

**Figure 10:** Comparing SiRAN with exhaustive assessment in terms of (a) performance and (b) computational overhead.

slices over no muting. However, it has 25% lower PF metric than SiRAN for the PF slices, with 19% of these slices having even worse performance than without muting. SOM-PF, in contrast, fares as well as SiRAN for the PF slices, but has 21% higher median FCT (or lower reduction in FCT) than SiRAN for the prioritized users in WPF slices.

*(iii) SiRAN vs RSEP:* RSEP underperforms SiRAN across the board in this scenario due to its channel agnostic slicing. It has 48% higher median FCT for the prioritized users in WPF slices when compared to SiRAN. It further achieves 39% lower throughput than SiRAN for the non-prioritized users in the WPF slices. For the PF slices, RSEP has 37.0% lower PF metric compared to SiRAN on an average, with almost 40% slices performing worse than RadioSaber no muting.

**Key Takeaway.** SiRAN's muting decisions benefit a substantial proportion of slices over RadioSaber (channel-aware slicing without muting), but *without penalizing* any other slice. In contrast, RSEP has inferior performance for many slices (even when compared to RadioSaber without muting) due to lack of channel-aware scheduling. SOM typically ends up penalizing slices with misaligned objective, thus breaking performance isolation across slices. Our results in Appendix E confirm the same trends as we vary number of users, slices and cells, and test settings with more than two categories of objectives. We also evaluate settings where slices have unequal quota across cells (SiRAN can deal with this naturally, while RSEP breaks in this setting).

## 6.3 Comparison w/ Exhaustive Assessment

In Fig. 10a we show how SiRAN (with its heuristics to assess benefit and cost of muting without repeatedly re-running the scheduler) compares against a variant that re-runs the schedulers for a more rigorous assessment (we refer to this variant as exhaustive assessment). We find that SiRAN's well-designed approximations produce no significant difference (+2.8%) in the outcome. For brevity, we only report a key result for scenario 3 – median FCT of prioritized users in WPF slices –(Fig. 10a), but trend holds more generally.

We use the software implementation (described in §5) on a single core to evaluate the runtime latency of both SiRAN and the exhaustive assessment baseline. Fig. 10b shows the results with 5G numerology 1 configuration (500$\mu$s TTI and 32 RBGs), four small cells and five slices. We vary the total number of users from 200 to 800 (3GPP standards recommend 200-400 number of users for a cluster of 1 macro-cell and four small cells [6]). We find that SiRAN's runtime latency comfortably fits within the TTI budget with up to 600 users. The exhaustive assessment approach, in contrast, exceeds the TTI budget even with 200 users. The exhaustive approach can potentially be parallelized to use more cores and reduce latency, but the increased cost and power might not be worth it given that SiRAN's approximations work as well (as shown in Fig. 10a). We repeat these experiments with varying numbers of cells, slices, and users, and for other 5G numerologies in Appendix D, confirming the same trends.

## 7 Concluding Remarks

In this paper, we present SiRAN, the first system that performs channel-aware RAN slicing across multiple cells while managing interference, maintaining isolation between slices and supporting customizable and diverse objectives within each slice. While our work focuses on downlink transmissions, we believe similar insights can also be applied to uplink. Moreover, we believe SiRAN's framework is not limited to muting alone, but can be applied more broadly to any coordination-based interference management scheme (we leave detailed exploration to future work).

## References


[1] A guide to 5G small cells and macrocells. https://www.essentracomponents.com/en-us/news/industries/telecoms-data/a-guide-to-5g-small-cells-and-macrocells.

[2] Cricket Wireless. https://www.cricketwireless.com/.

[3] FlexRAN Reference Architecture for Wireless Access. https://www.intel.com/content/www/us/en/developer/topic-technology/edge-5g/tools/flexran.html.

[4] Google Fi Wireless. https://fi.google.com/about/.

[5] Coordinated multi-point operation for lte physical layer aspects (3gpp release 11 3gpp tr 36.819 v11.2.0 2013-09). https://portal.3gpp.org/desktopmodules/Specifications/SpecificationDetails.aspx?specificationId=2498, 2013.

[6] Further advancements for e-utra physical layer aspects. Technical Report 36.814, 3rd Generation Partnership Project (3GPP), 2020. Version 9.0.0.

[7] 5G Data Traffic Explosion Will Drive 5G Small Cell Deployments to 13 million by 2027. https://www.abiresearch.com/press/5g-data-traffic-explosion-will-drive-5g-small-cell-deployments-to-13-million-by-2027, 2022.

[8] US cell towers and small cells: By the numbers. https://www.lightreading.com/digital-transformation/us-cell-towers-and-small-cells-by-the-numbers, 2022.

[9] 3rd Generation Partnership Project (3GPP). Physical Layer Procedures for Data. Technical Report TS 138 214, ETSI, 2021.

[10] R. Agrawal, A. Bedekar, S. Kalyanasundaram, N. Arulselvan, T. Kolding, and H. Kroener. Centralized and decentralized coordinated scheduling with muting. In *2014 IEEE 79th Vehicular Technology Conference (VTC Spring)*, pages 1–5, 2014.

[11] J. G. Andrews, S. Buzzi, W. Choi, S. V. Hanly, A. Lozano, A. C. K. Soong, and J. C. Zhang. What will 5g be? *IEEE Journal on Selected Areas in Communications*, 32(6):1065–1082, 2014.

[12] G. S. Association. 5g network slicing self-management white paper. https://www-file.huawei.com/-/media/corporate/pdf/news/5g-network-slicing-self-management-white-paper.pdf?la=en-us, 2020.

[13] G. Auer, V. Giannini, C. Desset, I. Godor, P. Skillermark, M. Olsson, M. A. Imran, D. Sabella, M. J. Gonzalez, O. Blume, and A. Fehske. How much energy is needed to run a wireless network? *IEEE Wireless Communications*, 18(5):40–49, 2011.

[14] N. Bhushan, J. Li, D. Malladi, R. Gilmore, D. Brenner, A. Damnjanovic, R. T. Sukhavasi, C. Patel, and S. Geirhofer. Network densification: the dominant theme for wireless evolution into 5g. *IEEE Communications Magazine*, 52(2):82–89, 2014.

[15] F. Boccardi, R. W. Heath, A. Lozano, T. L. Marzetta, and P. Popovski. Five disruptive technology directions for 5g. *IEEE Communications Magazine*, 52(2):74–80, 2014.

[16] P. Caballero, A. Banchs, G. de Veciana, and X. Costa-Pérez. Multi-tenant radio access network slicing: Statistical multiplexing of spatial loads. *IEEE/ACM Transactions on Networking*, 25(5):3044–3058, 2017.

[17] F. Capozzi, G. Piro, L. Grieco, G. Boggia, and P. Camarda. Downlink packet scheduling in lte cellular networks: Key design issues and a survey. *IEEE Communications Surveys Tutorials*, 15(2):678–700, 2013.

[18] Y. Chen, R. Yao, H. Hassanieh, and R. Mittal. Channel-Aware 5g RAN slicing with customizable schedulers. In *20th USENIX Symposium on Networked Systems Design and Implementation (NSDI 23)*, pages 1767–1782, 2023.

[19] E. Dahlman, S. Parkvall, and J. Sköld. Chapter 13 - multi-point coordination and transmission. In E. Dahlman, S. Parkvall, and J. Sköld, editors, *4G LTE-Advanced Pro and The Road to 5G (Third Edition)*, pages 331–345. Academic Press, third edition edition, 2016.

[20] M. Dirani, Z. Altman, and M. Salaun. Chapter 7 - autonomics in radio access networks. In N. Agoulmine, editor, *Autonomic Network Management Principles*, pages 141–166. Academic Press, Oxford, 2011.

[21] S. D'Oro, F. Restuccia, A. Talamonti, and T. Melodia. The slice is served: Enforcing radio access network slicing in virtualized 5g systems. In *IEEE INFOCOM*, page 442–450, 2019.

[22] Ericsson. Maximizing capacity in spectrum-limited networks. https://www.ericsson.com/en/reports-and-papers/microwave-outlook/articles/maximizing-capacity-in-spectrum-limited-networks, 2023.

[23] ETSI. 5G; 5G System; Network Slice Selection Services (3GPP TS 29.531 version 15.1.0 Release 15). https://www.etsi.org/deliver/etsi_ts/129500_129599/129531/15.01.00_60/ts_129531v150100p.pdf, 2018.

[24] ETSI. Evolved universal terrestrial radio access (e-utra); physical layer procedures. https://www.etsi.org/deliver/etsi_ts/136200_136299/136213/15.10.00_60/ts_136213v151000p.pdf, 2020.

[25] X. Foukas, M. K. Marina, and K. Kontovasilis. Orion: Ran slicing for a flexible and cost-effective multi-service mobile network architecture. In *Proceedings of the 23rd Annual International Conference on Mobile Computing and Networking*. Association for Computing Machinery, 2017.

[26] X. Foukas, G. Patounas, A. Elmokashfi, and M. K. Marina. Network slicing in 5g: Survey and challenges. *IEEE Communications Magazine*, 2017.

[27] S. Gulati, S. Kalyanasundaram, P. Nashine, B. Natarajan, R. Agrawal, and A. Bedekar. Performance analysis of distributed multi-cell coordinated scheduler. In *2015 IEEE 82nd Vehicular Technology Conference (VTC2015-Fall)*, pages 1–5, 2015.

[28] Y. Huang, S. Li, Y. T. Hou, and W. Lou. GPF: A GPU-Based Design to Achieve 100us Scheduling for 5G NR. In *Proceedings of the 24th Annual International Conference on Mobile Computing and Networking*. Association for Computing Machinery, 2018.

[29] R. Irmer, H. Droste, P. Marsch, M. Grieger, G. Fettweis, S. Brueck, H.-P. Mayer, L. Thiele, and V. Jungnickel. Coordinated multipoint: Concepts, performance, and field trial results. *IEEE Communications Magazine*, 49(2):102–111, 2011.

[30] V. Jungnickel, L. Thiele, T. Wirth, T. Haustein, S. Schiffermuller, A. Forck, S. Wahls, S. Jaeckel, S. Schubert, H. Gabler, C. Juchems, F. Luhn, R. Zavrtak, H. Droste, G. Kadel, W. Kreher, J. Mueller, W. Stoermer, and G. Wannemacher. Coordinated multipoint trials in the downlink. In *2009 IEEE Globecom Workshops*, pages 1–7, 2009.

[31] F. P. Kelly, A. K. Maulloo, and D. K. H. Tan. Rate control for communication networks: shadow prices, proportional fairness and stability. *J. Oper. Res. Soc.*, 49(3):237–252, 1998.

[32] R. Kokku, R. Mahindra, H. Zhang, and S. Rangarajan. Nvs: A virtualization substrate for wimax networks. In *Proceedings of the Sixteenth Annual International Conference on Mobile Computing and Networking*. Association for Computing Machinery, 2010.

[33] R. Kokku, R. Mahindra, H. Zhang, and S. Rangarajan. Nvs: A substrate for virtualizing wireless resources in cellular networks. *IEEE/ACM Trans. Network.*, oct 2012.

[34] R. Kwan, C. Leung, and J. Zhang. Proportional fair multiuser scheduling in lte. *IEEE Signal Processing Letters*, 2009.

[35] N. Lazarev, T. Ji, A. Kalia, D. Kim, I. Marinos, F. Y. Yan, C. Delimitrou, Z. Zhang, and A. Akella. Resilient baseband processing in virtualized rans with slingshot. In *Proceedings of the ACM SIGCOMM 2023 Conference*, ACM SIGCOMM '23, page 654–667, New York, NY, USA, 2023. Association for Computing Machinery.

[36] D. Lee, H. Seo, B. Clerckx, E. Hardouin, D. Mazzarese, S. Nagata, and K. Sayana. Coordinated multipoint transmission and reception in lte-advanced: deployment scenarios and operational challenges. *IEEE Communications Magazine*, 50(2):148–155, 2012.

[37] G. R. MacCartney and T. S. Rappaport. Millimeter-wave base station diversity for 5g coordinated multipoint (comp) applications. *IEEE Transactions on Wireless Communications*, 18(7):3395–3410, 2019.

[38] R. Mahindra, M. A. Khojastepour, H. Zhang, and S. Rangarajan. Radio access network sharing in cellular networks. In *2013 21st IEEE International Conference on Network Protocols (ICNP)*, pages 1–10, 2013.

[39] G. Manganaro and D. M. Leenaerts. *Advances in analog and RF IC design for wireless communication systems*. Academic Press, 2013.

[40] R. Misra, A. Gudipati, and S. Katti. Quickc: Practical sub-millisecond transport for small cells. In *Proc. ACM Mobicom*, page 109–121, 2016.

[41] R. Mittal, J. Sherry, S. Ratnasamy, and S. Shenker. Recursively Cautious Congestion Control. In *Proc. USENIX NSDI*, pages 373–385, 2014.

[42] L. Peterson and O. Sunay. *5G Mobile Networks: A Systems Approach*. USA, 2020.

[43] G. Piro, L. A. Grieco, G. Boggia, F. Capozzi, and P. Camarda. Simulating lte cellular systems: An open-source framework. *IEEE Transactions on Vehicular Technology*, 2011.

[44] R. Radjassamy. Think Small (Cell) to Go Big on 5G. RCR Wireless White Paper, 2021.

[45] O. D. Ramos-Cantor, J. Belschner, G. Hegde, and M. Pesavento. Centralized coordinated scheduling in lte-advanced networks. *EURASIP Journal on Wireless communications and Networking*, 2017(1):1–14, 2017.

[46] A. Rao. 5g network slicing: crossdomain orchestration and management will drive commercialization. https://www.cisco.com/c/dam/en/us/products/collateral/cloud-systems-management/network-services-orchestrator/white-paper-sp-5g-network-slicing.pdf, 2020.

[47] N. Saquib, E. Hossain, L. B. Le, and D. I. Kim. Interference management in ofdma femtocell networks: issues and approaches. *IEEE Wireless Communications*, 19(3):86–95, 2012.

[48] sharetech. Resource allocation type. https://www.sharetechnote.com/html/Handbook_LTE_RAType.html, 2020.

[49] ShareTechnote. 5g resource allocation types, 2024.

[50] M. U. A. Siddiqui, F. Qamar, F. Ahmed, Q. N. Nguyen, and R. Hassan. Interference management in 5g and beyond network: Requirements, challenges and future directions. *IEEE Access*, 9:68932–68965, 2021.

[51] S. Sun, Q. Gao, Y. Peng, Y. Wang, and L. Song. Interference management through comp in 3gpp lte-advanced networks. *IEEE Wireless Communications*, 20(1):59–66, 2013.

[52] Unknown. Moving 5g spectrum to a shared resource. https://www.rcrwireless.com/20170404/5g/20170404analyst-anglemoving-5g-spectrum-shared-resource, apr 2017. Accessed: 2024-04-28.

[53] C. Wengerter, J. Ohlhorst, and A. von Elbwart. Fairness and throughput analysis for generalized proportional fair frequency scheduling in ofdma. In *2005 IEEE 61st Vehicular Technology Conference*, pages 1903–1907 Vol. 3, 2005.

[54] Y. Xie and K. Jamieson. Ng-scope: Fine-grained telemetry for nextg cellular networks. *Proc. ACM Meas. Anal. Comput. Syst.*, 6(1), feb 2022.

[55] J. Xing, J. Gong, X. Foukas, A. Kalia, D. Kim, and M. Kotaru. *Enabling Resilience in Virtualized RANs with Atlas*. Association for Computing Machinery, New York, NY, USA, 2023.

[56] Y. Zhou, L. Liu, H. Du, L. Tian, X. Wang, and J. Shi. An overview on intercell interference management in mobile cellular networks: From 2g to 5g. In *2014 IEEE International Conference on Communication Systems*, pages 217–221, 2014.

# Appendix

## A Importance of Small Cells and Frequency Sharing

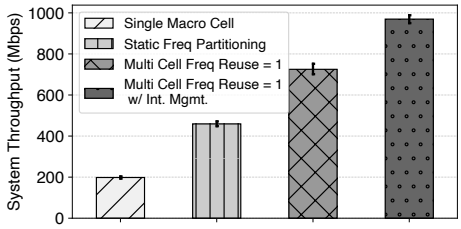


**Figure 11:** System throughput under different frequency allocation strategies

**Frequency Sharing.** A key design decision in multi-cell deployments concerns how to partition the radio frequency among cells. One option is to partition the frequency statically, ensuring that neighboring cells never transmit at the same frequency and thus avoid interference. However, this approach leads to inefficient spectrum usage, reducing the usable bandwidth for each cell. An alternative is to allow neighboring cells to share the same frequency band (frequency reuse one). This introduces the challenge of managing interference that would arise when two cells transmit simultaneously on the same frequency, degrading the channel quality users in the overlapping coverage regions of both cells. Nonetheless, dynamically managing interference (depending on when which users suffer from it) still results in better resource utilization and overall system performance compared to statically partitioning radio frequency among cells. These performance benefits of frequency reuse are well-known [20, 22], making it a preferred deployment choice in many settings [52].

To understand the significance of these choices, we conduct a simple experiment, starting with 150 users, attached to a single macro-cell, randomly distributed within its range. We next introduce 4 small cells into the macro-cell's coverage region, but statically partition the frequency (reserving 50% of the bandwidth for the macro-cell, with the remaining 50% used by small cells). This results in 100% higher throughput compared to single cell setting. We next evaluate the multi-cell setup under frequency re-use one, where the entire frequency band is shared across cells. This improves throughput by 70% over the static partitioning setup. Dynamically conducting interference management using the muting strategy described in §3.2 (for throughput maximization objective) further improves throughput by an additional 35%.

## B Channel Quality Information for Muting

Assessment of muting decisions require knowing the channel quality of users with and without interference. 5G New Radio (NR) scheduling allows for the configuration of a set of Resource Elements (REs)—smaller individual subcarriers within an RBG—to be dedicated for the purpose of interference measurement, known as the Channel State Indicator Interference Measurement Resource (CSI-IM) [9]. Coordinating cells periodically co-schedule known reference symbols and zero-power symbols sequentially, based on the Channel Feedback interval (typically 40 ms), to achieve accurate per-cell interference values. For example, on Resource Element $r_i$, Cell $C_j$ would transmit a known Reference Symbol while Cell $C_{j+1}$ to $C_n$ would schedule a Zero Power Reference Symbol (ZP-CSI-RS); here, Cell $C_j$ is transmitting and creating interference, while all other cells are 'quiet' and only measuring the interference created by Cell $C_j$ [19]. This process is iteratively repeated by all the cells in the coordinating cluster—one cell transmitting and the rest remaining quiet on those REs and measuring the transmitter's interference—to achieve accurate interference values. This measurement is cost-effective since only a subset of an RBG (typically 2 out of 48 REs per RBG) are allocated for CSI-IM, allowing normal data transmission on all remaining REs of the RBG.

## C Details about SiRAN's Cost Computation

We take the scores associated with each RBG allocated to a given slice at a given cell under the initial allocation (mentioned in §4.3), and group these RBGs into clusters. Our clustering logic is cheap and simple – we compute the average score ($\mu$) and the standard deviation ($\sigma$) across all RBGs allocated to the slice, and cluster them into atmost five sets – RBGs with scores (i) $\leq (\mu - 2\sigma)$, (ii) $> (\mu - 2\sigma)$ and $\leq (\mu - \sigma)$, (iii) within $(\mu \pm \sigma)$, (iv) $\geq (\mu + \sigma)$ and $< (\mu + 2\sigma)$, and (v) $\geq (\mu + 2\sigma)$.

We then compute the average score within each cluster, and use them to assess the worth of an RBG. Suppose the cluster with lowest score for a given slice $S_k$ at cell $C_j$ has $n$ RBGs and an average score of $X$. As long as the total quota reduced from slice $S_k$ due to muting at $C_j$ remains less than $n$ RBGs, we associate a worth of $X$ for each RBG (so a quota reduction of 0.5RBGs will incur a cost of $0.5X$). Once the quota reduction for $S_k$ exceeds $n$ RBGs (due to muting decisions made over multiple RBGs), we move over to considering the cluster with the next lowest average score, and so on. The clustering avoids excessive overfitting to the specific RBG scores in the initial hypothetical allocation, which are subject to change as muting decisions take place over RBGs.

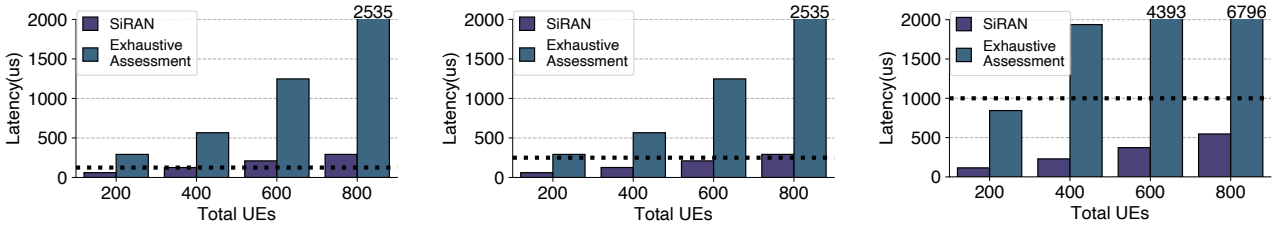


**(a)** TTI = 125 **(b)** TTI = 250 **(c)** TTI = 1000

**Figure 12:** The runtime latency of SiRAN and the exhaustive assessment approach with 5G numerology 0, 2, and 3. The corresponding TTIs are 125us, 250us, and 1000us.

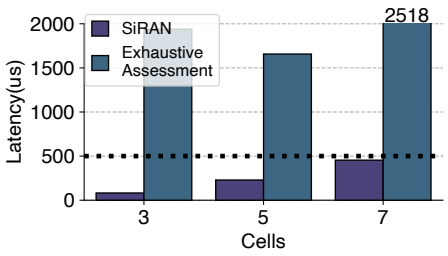


**(a)** Latency with Different Cells

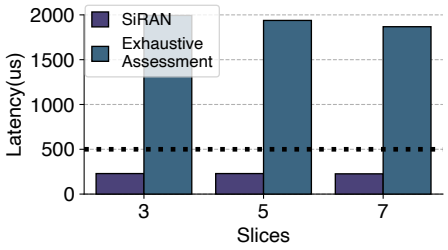


**(b)** Latency with Different Slices

**Figure 13:** The runtime latency of SiRAN and the exhaustive-assessment baseline with different number of cells and slices

## D Runtime Overhead

Now we discuss how the numerology, the number of small cells, and the number of slices affect the runtime latency of both SiRAN and the exhaustive assessment baseline. In the first experiment, we have five slices and five cells(same configuration in §6.3), and evaluate both systems with 5G numerology 0(32RBGs, 1000us TTI), 2(16RBGs, 250us TTI), and 3(16RBGs, 125us TTI). Figure12 shows the runtime latency of both systems with different number of users. We can see the runtime latency of the exhaustive baseline is well above one TTI in all numerology configurations with only 400 users. Nevertheless, SiRAN can support up to 600 users in numerology 0, 2, and up to 400 users in numerology 3. This concludes that SiRAN can be practical with most 5G numerology configurations nowadays.

Then we'll understand how the number of slices and the number of cells affect the scheduling latency. In the following experiments, we fix the total number of users to 400 and use numerology 1. Fig. 13a shows that the runtime latency increases as the number of cells increases since it requires more coordination between cells. SiRAN can support up to 6 small cells. Fig. 13b shows that the number of slices doesn't have obvious impact on the runtime latency. However, the runtime latency of the exhaustive baseline is again well above one TTI.

## E Additional Evaluation:

To further demonstrate the robustness of SiRAN, we conduct additional experiments by varying parameters such as number of cells, users and slices. The results of these experiments are summarized below.

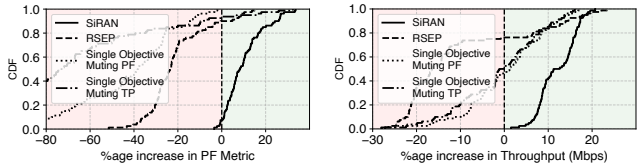


**(a)** Per slice performance of PF slices **(b)** Per slice performance of MT slices

**Figure 14:** SiRAN 's, RSEP's and SOM-PF's and SOM-TP's impact on slice-level performance when compared to RadioSaber (no muting) for (a) PF slices and (b) Max TP slices under Scenario 2 with unequal slice quotas and distribution across cells.

### E.1 Varying Quota Across Cells

The traffic parameters for this experiment remain the same as those described in Section 6.2, Table 7a. The key difference is that approximately 75% of the users in the Max Throughput slices are now attached to the Macro Cell, with only 25% attached to the Small Cells. As a result, the quota of the Max

Throughput slices gets increased proportionally at the Macro Cell and reduced at the Small Cells. Conversely, for the Proportional Fairness slices, the distribution is reversed, with 75% of users attached to the Small Cells and the remaining 25% to the Macro Cell. The results are shown in Figure 14.
*(i) SiRAN vs RadioSaber without muting:* SiRAN continues to demonstrate its effectiveness, offering a mean improvement of 10.2% in the PF metric for PF slices, while maintaining slice-level isolation with near-zero loss across all slices (approximately 5% of slices experience a minor mean loss of 1.5%). For MT slices, SiRAN provides a 12.8% improvement in throughput, again ensuring no performance degradation for any slice.
*(ii) SiRAN vs SOM:* Under this unequal distribution, both variants of SOM—configured with either the PF or MT metric—fail to perform well on their respective metrics, breaking slice-level isolation and degrading performance for most slices - 90% of all slices under SOM-PF and 50% of all slices under SOM-MT see a reduction in their slice level metric than compared to the no muting baseline. This failure stems from the increased likelihood of having non-matching metrics across cells. For example, when SOM-PF attempts to maximize the PF metric globally across all cells, it inadvertently includes the PF contributions of users from MT slices in its global optimization decisions. Since these users inherently prioritize throughput over fairness, their inclusion distorts the PF metric, resulting in poorly informed decisions that harm slice-level objectives. Similarly, SOM-MT faces a similar issue: by trying to globally maximize throughput, it incorporates MT contributions from PF users, whose scheduling decisions focus on fairness rather than throughput. This mismatched metric aggregation leads to suboptimal global optimization and significantly impacts the individual objectives of the slices.
*(iii) SiRAN vs RSEP:* The unequal distribution exacerbates mismatches between RBs across cells, breaking RSEP's RB-linkage rule. This prevents RSEP from effectively managing interference on those RBs, further compounded by its channel-unaware allocation mechanism. As a result, 90% of all PF slices and 76% of all MT slices experience degraded performance compared to the no muting baseline.

## E.2 Varying Number of Slices

In this scenario (summarized in Table 15a), we increase the number of slices to 12, consisting of three categories: PF slices (4 slices) optimizing for proportional fairness ($\alpha = 1$), MT slices (4 slices) optimizing for throughput, and WPF slices (4 slices) using a weighted proportional fairness objective. The WPF slices assign a high weight (1000) to 40% of randomly selected users following a web flow traffic pattern, while the remaining 60% of users have a weight of 1 and follow a backlogged traffic pattern.
*(i) SiRAN vs RadioSaber without muting:* SiRAN maintains its trend of ensuring slice-level isolation, providing targeted performance improvements across slices while incurring minimal loss (only a small subset of MT slices see a slight −5% drop in performance). For the PF slices, SiRAN improves the PF metric by an average of 86%, while for the MT slices, it increases throughput by 12%. Among WPF slices, it reduces the median FCT of prioritized internet flows by 27%.
*(ii) SiRAN vs SOM:* We evaluate all three SOM variants, each optimizing a different global objective (PF, MT, WPF). As seen in previous scenarios, SOM benefits slices aligned with its chosen metric but imposes severe penalties on others. - SOM-PF improves the PF metric by 72% (14% lower than SiRAN) while limiting performance degradation to only 5% of the slices. However, it performs poorly for MT slices, offering only a 0.3% throughput improvement (11.3% lower than SiRAN) while degrading 49% of the slices. - SOM-WPF reduces the median FCT of prioritized internet flows by 30% but severely impacts MT slices, decreasing throughput for 80% of them by an average of -5%, with some slices experiencing drops as large as -19%. - SOM-MT performs well for MT slices, improving throughput by 39%, but drastically degrades the PF slices, reducing their PF metric by an average of -200%, as seen in Fig. 15b. It also increases median FCT by up to 500%, and we omit its results from Fig. 15d to avoid distorting the figure.
*(iii) SiRAN vs RSEP:* Due to its channel-unaware scheduling, RSEP consistently underperforms compared to SiRAN. It provides only a 6% improvement for PF slices (80% lower than SiRAN) while degrading 21% of slices. It further reduces the average throughput of MT slices by -5% and offers only a 13% median FCT improvement (14% lower than SiRAN).

## E.3 Varying Users and Cells

To evaluate the scalability and consistency of SiRAN 's performance, we vary the number of users and cells while keeping the traffic parameters controlled, as described in Table 9a. The results, summarized in Fig. 16, confirm that the trends observed in Section 6 hold across different configurations, demonstrating that SiRAN maintains its effectiveness under varying physical network configurations. For brevity, we only include the results for the median reduction in the FCT of prioritized web flow traffic but the trends hold across other groups of users as well.

## E.4 Design Justifications

To evaluate the impact of our system optimizations discussed in Section §6, we measure system performance in their absence. We use the same underlying traffic distribution (but with static users) as in Table 9a and record the reduction in median FCT for the prioritized web flows. The results are reported in Fig. 17.

| Parameter | PF Slices | TP Slices | WPF Slices |
|---|---|---|---|
| # Slices | 4 | 4 | 4 |
| Traffic Pattern | Backlogged | Backlogged | •40% Web Flow ($W$ = 1000x)<br>•60% Backlogged |
| Objective | PF | Max Throughput | Weighted PF |
| Metric | $\sum_i \log x_i$ | avg tpt | Median FCT |
| Result | Fig. 15b | Fig. 15c | Fig. 15d |

**(a)** Slice Level Metrics for Appendix E.2

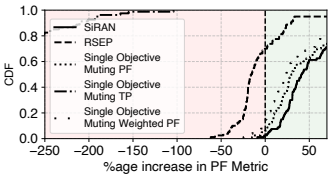


**(b)** Per slice performance for PF-slices

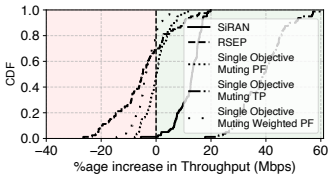


**(c)** Per slice performance for MT-slices

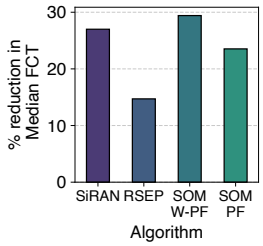


**(d)** % reduction in median FCT for internet flows

**Figure 15:** SiRAN's, RSEP's and SOM's impact on slice-level performance when compared to RadioSaber (no muting) for the (b) PF slices (b) MT slices and (c) Weighted PF Slices

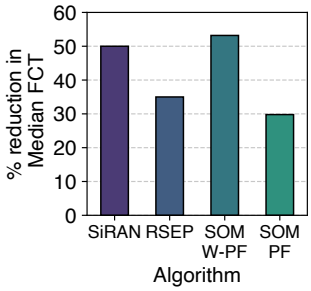


**(a)** 160 users, 3 cells

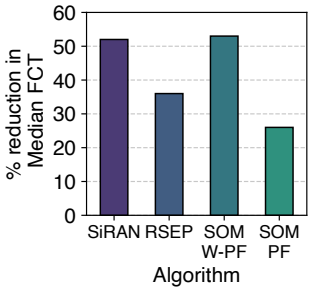


**(b)** 160 users, 4 cells

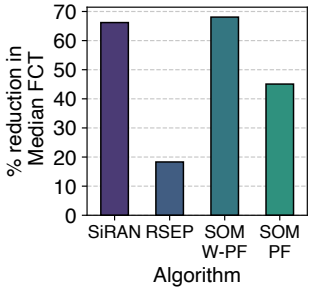


**(c)** 160 users, 5 cells

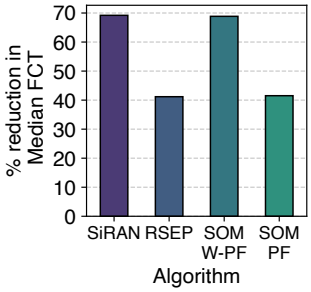


**(d)** 240 users, 5 Cells

**Figure 16:** SiRAN's, RSEP's and SOM W-PF's and SOM-PF's impact on median FCT for prioritized web flows when compared to RadioSaber (no muting), across varying physical network parameters.

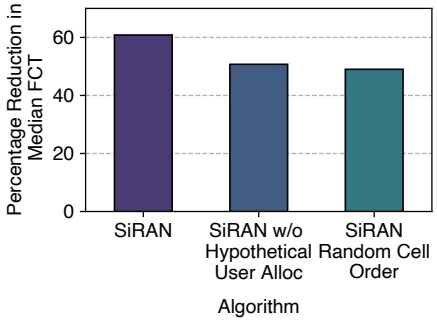


**Figure 17:** Impact of SiRAN system optimizations on Median FCT

**Impact of hypothetical baseline when computing benefit.** SiRAN computes the benefit of muting by comparing the user score a slice achieves at a neighboring cell with a hypothetical allocation where we compute the score that the same slice would have achieved on the same RBG without muting. We try a variant where we directly use the score achieved by a slice at a neighboring cell without subtracting the score from this hypothetical baseline. We find that it produces notably smaller reduction in median FCT of prioritized users (10% lower than original SiRAN) when compared to our original design (Fig. 17 first bar from the left).

**Impact of cell selection heuristic.** With multiple valid muting hypothesis across cells, SiRAN selects one based on benefit-cost ratio across the set of benefitting slices and side-effect on other slices. We implement a variant where we randomly select a hypothesis (which cell to mute) among multiple valid ones. This simplified variant again produces a notably smaller reduction in median FCT (11% lower than our original design as shown in Fig. 17), justifying the usefulness of our optimizations in this context.

# F SiRAN Algorithm

The following algorithms outline the implementation logic of the SiRAN system.

- At the heart of SiRAN lies a novel cost-benefit trade-off algorithm, which determines the benefit for each slice based on its unique metric. It assigns the cost of muting exclusively to the slices that benefit from the interference management decision. This logic is captured in Algorithm 1, corresponding to the explanation in Section 4.1.
- Algorithm 2 describes the muting logic, where each cell is evaluated for muting at every RBG. The net

benefit of each muting decision is computed based on the logic detailed in Section 4.2.

- To accurately assess the cost for each slice, the system estimates the average performance of each slice at every cell for a single RBG. This heuristic informs the cost-benefit tradeoff process. The algorithm, executed once per TTI, is summarized in Algorithm 3 and further explained in Section 4.3.

**Algorithm 1** `PerSliceCostBenefitTradeoff(S)` (Called by `ConsiderMutingHypothesis`)

**Input:** $benefitting\_slices$
**Output:** Updated $benefitting\_slices$ and $benefit\_ratio$

Initialize $benefit\_ratio \leftarrow 0$
**while** True **do**
  $changes \leftarrow$ False
  **for** each $s$ in $benefitting\_slices$ **do**
    **if** Net Benefit$_s$ $<$ Avg Performance$_s$ $\times \frac{1}{\text{len}(benefitting\_slices)}$ **then**
      Remove $s$ from $benefitting\_slices$
      Reset $benefit\_ratio \leftarrow 0$
      $changes \leftarrow$ True
      **break**
    **else**
      $benefit\_ratio \leftarrow benefit\_ratio + \frac{\text{Net Benefit}_s}{\text{Avg Performance}_s \times \frac{1}{\text{len}(benefitting\_slices)}}$
    **end if**
  **end for**
  **if** not $changes$ **then**
    **break**
  **end if**
**end while**
**return** $benefit\_ratio$

**Algorithm 2** `ConsiderMutingHypothesis(RBG_R_i)`

Initialize $S \leftarrow \emptyset$ *Set of slices that benefit from muting*
Initialize `max_benefit_ratio` $\leftarrow 0$
Initialize `best_muting_option` $\leftarrow$ None
**for** each $i$ in cells **do**
  Mute $i$
  `Sched_Mute` $\leftarrow$ Schedule across all Cells under Muting *(Store Schedule for Muted State)*
  `Sched_NoMute` $\leftarrow$ Schedule across all Cells without Muting *(Store Schedule for Non-Muted State)*
  **for** each Slice $s$ **do**
    Compute Metric under Muting using `Sched_Mute`
    Compute Metric without Muting using `Sched_NoMute`
    Net Benefit $\leftarrow \sum_{c=0}^{|\text{cells}|}$ Metric under Muting
      $- \sum_{c=0}^{|\text{cells}|}$ Metric without Muting
    **if** Net Benefit $> 0$ **then**
      Add $s$ to $S$
    **end if**
  **end for**
  `current_benefit_ratio` $\leftarrow$ `PerSliceCostBenefitTradeoff`$(S)$
  **if** `current_benefit_ratio` $>$ `max_benefit_ratio` **then**
    `max_benefit_ratio` $\leftarrow$ `current_benefit_ratio`
    `best_muting_option` $\leftarrow i$
  **end if**
**end for**
**if** `max_benefit_ratio` $== 0$ **then**
  **Return:** No Muting
**else**
  Apply Muting to `best_muting_option`
**end if**

**Algorithm 3** `ComputeAveragePerformanceForEachSlice()`

Perform Complete Allocation across all RBGs under no muting
Initialize Total Metric$[S] \leftarrow 0$ and RBG Count$[S] \leftarrow 0$ for all slices $S$
**for** each RBG $R$ **do**
  Let $S_R \leftarrow$ Slice allocated to RBG $R$
  Metric Achieved $\leftarrow$ Metric$_{S_R,R}$ {Performance metric for $S_R$ on $R$}
  Total Metric$[S_R] \leftarrow$ Total Metric$[S_R]$ + Metric Achieved
  RBG Count$[S_R] \leftarrow$ RBG Count$[S_R] + 1$
**end for**
**for** each Slice $S$ **do**
  **if** RBG Count$[S] > 0$ **then**
    Avg Performance$_S \leftarrow \frac{\text{Total Metric}[S]}{\text{RBG Count}[S]}$
  **end if**
**end for**